Engineered allosteric mutants of the integrin αMβ2 I domain: structural and functional studies

Clare J. McCLEVERTY and Robert C. LIDDINGTON[1]

The Burnham Institute, 10901 North Torrey Pines Rd, La Jolla, CA 92037, U.S.A.

The α-I domain, found in the α-subunit of the leucocyte integrins such as αMβ2 and αLβ2, switches between the open and closed tertiary conformations, reflecting the high- and low-affinity ligand-binding states of the integrin that are required for regulated cell adhesion and migration. In the present study we show, by using point mutations and engineered disulphide bonds, that ligand affinity can be reduced or increased allosterically by altering the equilibrium between the closed and open states. We determined equilibrium constants for the binding of two ligands, fibrinogen and intercellular cell-adhesion molecule 1, to the αM-I domain by surface plasmon resonance, and determined crystal structures of a low-affinity mutant. Locking the domain in the open conformation increases affinity by a factor of no greater than 10, consistent with a closely balanced equilibrium between the two conformations in the absence of ligand. This behaviour contrasts with that of the unliganded αL-I domain, for which the equilibrium lies strongly in favour of the closed conformation. These results suggest significant differences in the way the parent integrins regulate I domain conformation and hence ligand affinity.

Key words: A domain, allostery, gain-of-function, I domain, integrin.

INTRODUCTION

Integrins are adhesion receptors that mediate cell adhesion and migration by binding extracellular matrix (or counter-receptors on other cells) via their extracellular heads, and cytoskeletal and signalling molecules via their cytoplasmic tails [1]. They are αβ heterodimers, consisting of a head domain from which emerges two legs, one from each subunit, ending in a pair of single-pass transmembrane helices and short cytoplasmic tails (Figure 1A). The integrin 'head' comprises a seven-bladed propeller from the α-subunit that makes an intimate contact with a GTPase-like domain of the β-subunit (the β-I domain), in a manner that resembles the heterotrimeric G proteins [2]. Nine α-subunits (α1, α2, α10, α11, αD, αE, αL, αM and αX) contain an additional domain, the α-I domain, that is inserted between two loops on the upper surface of the propeller, where it plays a central role in ligand binding [3–5]. Instead of a catalytic centre, the I domain contains an invariant ligand-binding site called MIDAS, for metal-ion-dependent adhesion site, in which a metal ion is co-ordinated by three loops from the I domain, and a glutamic or aspartic acid from the ligand completes an octahedral co-ordination sphere around the metal (Figure 1B). In those integrins that lack an α-I domain, the β-I domain and propeller are major ligand recognition sites [6]; in the α-I domain integrins, the β-I domain and propeller play regulatory roles. In the absence of ligand, bonds between the legs, tails and head are believed to hold the head in an 'inactive' or 'resting' conformation that has low affinity for ligand [7–9]. Recent structural data suggest that this conformation is severely bent [10], in contrast to the extended conformation assumed from earlier studies. During 'outside-in' signalling, the head binds to extracellular matrix proteins or counter-receptors on other cells, triggering a 'switchblade' opening of the integrin head that is propagated down the 'legs' and through the plasma membrane, leading to a re-organization of the C-terminal tails that allows them to bind intracellular proteins [10,11]. During 'inside-out' signalling, cytosolic proteins bind and sequester one or both of the cytoplasmic tails, triggering conformational changes in the head that lead to a high-affinity 'active' integrin [9,12].

The first α-I domain crystal structure, from integrin αMβ2, revealed a compact domain comprising a central mostly parallel β-sheet surrounded on both sides by amphipathic α-helices [13] (Figure 1B). The invariant MIDAS motif lies at the C-terminal end of the central β-sheet, with three loops contributing side chains that co-ordinate the Mg^{2+} ion. Surface-exposed side chains surrounding the MIDAS motif are variable; they provide additional ligand contact points and hence ligand specificity [3,14–22]. The crystal structure of the α2-I domain, in complex with a triple helical fragment of collagen, provides a model for ligand engagement by all α-I domains [23]. A glutamic acid side chain from the ligand completes the co-ordination sphere of the Mg^{2+}, while further specificity arises from contacts with the surrounding surface. This structure, along with an earlier structure of the αM-I domain bound to a 'ligand-mimetic' crystal contact [24], demonstrates that ligand binding triggers a profound conformational switch in the α-I domain that underlies affinity regulation and signal transduction.

Recombinant I domains exist in two distinct conformations, open (high affinity) and closed (low affinity) (Figure 1B). The key difference between these conformations is the rearrangement of the metal-co-ordinating residues at the MIDAS, allowing the ligand glutamate to bind, which is mechanically coupled to a large downward shift of the C-terminal helix at the opposite pole of the domain. The shift of the C-terminal helix is highly significant in the context of the whole integrin, since the helix is packed

Abbreviations used: DTNB, 5,5′-dithiobis-(2-nitrobenzoic acid); DTT, dithiothreitol; EDC, *N*-ethyl-*N*′-(3-dimethylaminopropyl)carbodiimide hydrochloride; G127-I319 mutant etc., mutation of residue Gly-127 → Ile-319 etc.; ICAM-1, intercellular cell-adhesion molecule 1; K_D, partition coefficient; MIDAS, metal-ion-dependent adhesion site; NHS, *N*-hydroxysuccinimide; sICAM-1, soluble ICAM-1; SPR, surface plasmon resonance.

[1] To whom correspondence should be addressed (e-mail rlidding@burnham.org).

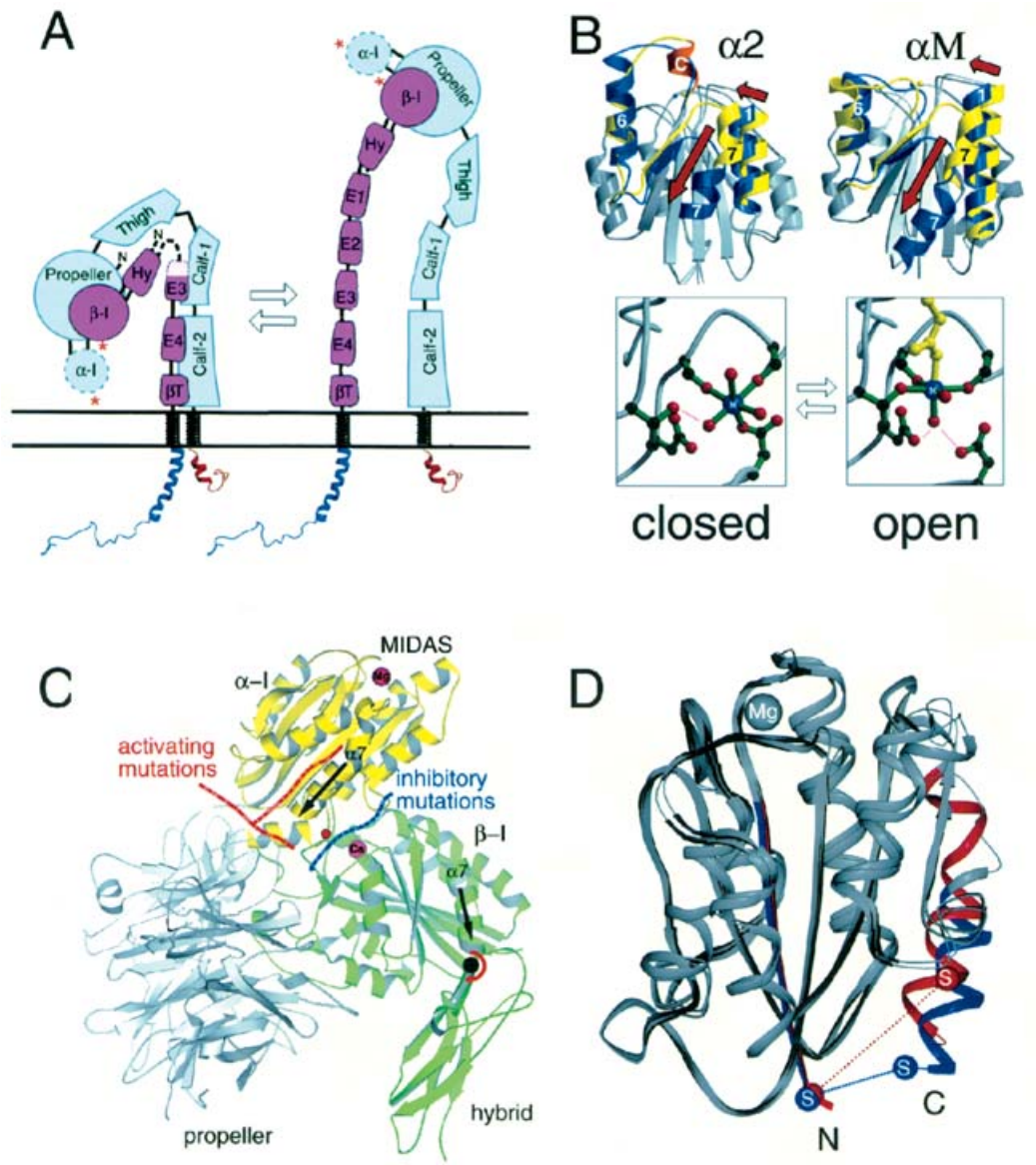

Figure 1 Integrin allostery and experimental design

(**A**) Domain organization of an integrin, derived from crystallographic, electron microscopy and NMR studies [2,9,10]. Upon activation, the integrin 'stands up', releasing constraints on the head domains (α-I, β-I and propeller) and leading to a separation of the legs and tails. (**B**) Two conformations of the α-I domain. The upper panels compare open and closed forms of the α2-I (α2) [23] and αM-I (αM) [24] domains, with red arrows indicating major conformational changes. Regions that undergo large structural changes are shown in blue (open/liganded) and yellow (closed/unliganded). The lower panels detail the MIDAS motif in the closed and open (ligand-bound) conformations. (**C**) Hypothetical model of the αMβ2 head piece, based on the αVβ3 [2] and αM-I [24] crystal structures. Surfaces that lead to activation (gain-of-function) and inhibition (loss-of-function) when mutated are indicated. The proposed axis about which the β-I domain rotates on activation [37] is indicated by a black circle. (**D**) Design of an engineered disulphide bridge that stabilizes the open conformation of the αM-I domain. Blue represents the open state and red the closed state, with the metal at the MIDAS shown as a grey sphere (Mg). Engineered cysteines (D132C and K315C) are indicated (S). The disulphide can only form in the open conformation.

against the propeller and β-I domain. How does the quaternary organization of the integrin control the conformation of the α-I domain, and hence, ligand affinity? To begin to shed light on this issue, we have introduced point mutations and engineered disulphide bonds into the αM-I domain to stabilize the open and closed conformations, and determined binding constants for two ligands, intercellular cell-adhesion molecule 1 (ICAM-1) and fibrinogen. Our studies show that the equilibrium between the recombinant αM and αL-I domain conformations is very different, with distinct implications for how the parent integrin regulates ligand affinity.

MATERIALS AND METHODS

Mutagenesis

Site-directed mutagenesis was carried out in a pGEX-2T vector, encoding residues Gly-127 → Ile-319 (G127–I319) of the recombinant αM-I domain (provided by GlaxoSmithKline, Stockley Park West, Uxbridge, Middlesex, U.K.). Mutations were generated using the QuikChange Site-Directed Mutagenesis kit (Stratagene, La Jolla, CA, U.S.A.) with the following substitutional mutagenic primers: C128A forward, 5′-GAGGCCCT-CCGAGGGGCTCCTCAAGAGGATAGTG-3′; C128A reverse,

5′-CACTATCCTCTTGAGGAGCCCCTCGGAGGGCCTC-3′; C128A-D132C forward, 5′-GCTCCTCAAGAGTGTAGTGAC-ATTGCC-3′; C128A-D132C reverse, 5′-GGCAATGTCACTAC-ACTCTTGAGGAGC-3′; L164F forward, 5′-ACTGTGATGGA-GCAATTCAAAAAGTCCAAAACC-3′; L164F reverse, 5′-GG-TTTTGGACTTTTTGAATTGCTCCATCACAGT-3′; F302W forward, 5′-TTCCAGGTGAATAACTGGGAGGCTCTGAAG-ACC-3′; F302W reverse, 5′-GGTCTTCAGAGCCTCCCAGTTA-TTCACCTGGAA-3′; E314R–K315C forward, 5′-CAGAACC-AGCTTCGGAGGTGTATCTTTGCGATCG-3′; E314R–K315C reverse, 5′-CGATCGCAAAGATACACCTCCGAAGCTGGTT-CTG-3′; K315C forward, 5′-AACCAGCTTCGGGAGTGTAT-CTTTGCGATCGG-3′; K315C reverse, 5′-CCGATCGCAAAG-ATACACTCCCGAAGCTGGTT-3′; I316R forward, 5′-CAGC-TTCGGGAGAAGAGGTTTGCGATCGGATCC-3′; I316R re-verse, 5′-GGGATCCGATCGCAAACCTCTTCTCCCGAAGC-TG-3′ A318C forward, 5′-CGGGAGAAGATCTTTTGCATCG-GATCCCCGGG-3′; A318C reverse, 5′-CCCGGGGATCCGAT-GCAAAAGATCTTCTCCCG-3′.

Introduction of the respective mutations was confirmed by direct DNA sequencing.

Protein preparation

The wild-type and mutant αM-I domains were expressed as glutathione S-transferase (GST)-fusion proteins in *Escherichia coli* as described previously [3]. The I domain was digested overnight at 4 °C with 0.5 % (w/w) immobilized trypsin (Pierce, Rockford, IL, U.S.A.) to remove 16 N-terminal residues that interfere with crystal growth. The free cysteine in wild-type αM-I domain was blocked with iodoacetamide after reduction to prevent dimer formation. The C128A/D132C/K315C mutant was incubated with 0.1 mM $CuSO_4$ and 0.1 mM *o*-phenanthroline to promote disulphide bond formation. The presence of free cysteines was determined by titration against DTNB [5,5′-dithiobis-(2-nitrobenzoic acid)] in 6 M guanidinium hydrochloride/20 mM Tris/HCl, pH 8.0, using L-cysteine to generate a calibration curve. Wild-type and mutant I domains were assessed for monomer formation by size-exclusion chromatography on a 24-ml-Superdex-75 column HR 10/30 using the AKTA system (Amersham Pharmacia Biotech, Piscataway, NJ, U.S.A.). Recombinant soluble ICAM-1 (sICAM-1) containing all five extracellular immunoglobulin domains (D1–D5) was provided by GlaxoSmithKline and fibrinogen was a gift from Dr R. F. Doolittle (University of California, San Diego, CA, U.S.A.).

Surface plasmon resonance (SPR) studies

A Biacore 3000 SPR-based biosensor (Biacore AB, Uppsala, Sweden) was used to measure binding parameters for the interaction between the αM-I domain and the ligands, fibrinogen and sICAM-1. All proteins were dialysed extensively against running buffer containing 20 mM Hepes, 150 mM NaCl, 0.005% polysorbate 20, 5 mM $MgCl_2$, pH 7.5. sICAM-1 and fibrinogen were immobilized, at concentrations ranging from 200 to 1000 response units, onto Pioneer B1 chips (Biacore) via *N*-ethyl-*N*′-(3-dimethylaminopropyl)carbodiimide hydrochloride (EDC)/*N*-hydroxysuccinimide (NHS) cross-linking as directed by the manufacturer. A blank flow cell which had been EDC/NHS activated and ethanolamine blocked was used as a reference surface. Steady-state experiments were performed by injecting the I domains over the chip at 5 $\mu l \cdot min^{-1}$ for 8 min. The chip surface was regenerated with 1 M NaCl. Typically, sensorgrams

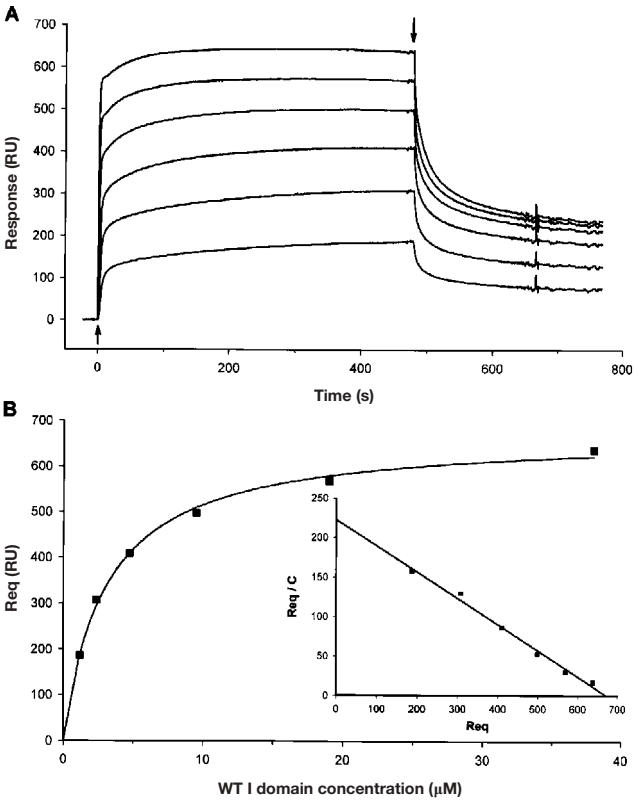

Figure 2 Equilibrium analysis of the interaction of wild type αM-I domain with fibrinogen

(**A**) Sensorgram overlays for I domain concentrations ranging from 38 μM to 1.2 μM (from top to bottom) binding to fibrinogen immobilized on the chip surface. The beginning and end of injections are shown with an arrow. (**B**) Saturable binding curve and Scatchard plot (inset). The K_D value calculated for this experiment was 3.12 μM. Req is the response at equilibrium. RU, response units; WT, wild-type.

were obtained at six different concentrations for each experiment, and each set of titrations included a running buffer injection to be used as an additional blank. All data were analysed using the BIAevaluation 3.0 program, subtracting binding to the blank flow cell and the blank buffer injection to account for any non-specific binding. For each sensorgram, the peak response levels achieved in the steady-state region were plotted against analyte concentration. This plot was fitted to a single-site-binding equation (Langmuir isotherm) to determine dissociation constant (K_D) values (Figure 2).

Crystallographic studies of wild-type, A318C and reduced C128A/D132C/K315C αM-I domain mutants

The wild-type and mutant proteins were dialysed into 100 mM NaCl, 5 mM $MgCl_2$, 20 mM Tris, pH 8.0, and concentrated to 10 mg/ml prior to crystallization. All crystals were grown using the sitting-drop vapour diffusion method. Wild-type crystals were grown using 0.2 M NaCl, 20% poly(ethylene glycol) 8000, 0.1 M potassium citrate, pH 4.2, at 23 °C. A318C crystals grew using 22%–30% (w/v) poly(ethylene glycol) monomethyl ether 2000, 0.2 M $(NH_4)_2SO_4$, 0.1 M sodium acetate, pH 4.6, at 4 °C. Reduced C128A/D132C/K315C crystals grew using 0.2 M NaCl, 20% poly(ethylene glycol) 3000, 0.1 M Hepes, pH 7.5, at 23 °C. All crystals were soaked in reservoir buffer containing 20% (v/v) glycerol and flash-frozen in a cryo-stream of nitrogen at 100 K. Data from wild-type and A318C crystals

Table 1 Summary of crystallographic data

RMSD, root-mean-square deviation.

Diffraction data	Wild-type	A318C	Reduced C128A/D132C/K315C
Space group	$P2_12_12_1$	$P2_12_12_1$	$P4_3$
Unit cell dimensions (Å)			
a	38.4	38.6	44.2
b	50.9	51.0	44.2
c	102.4	102.4	99.9
Resolution (Å)	1.5	1.25	2.5
Number of observations	125 137	170 186	14 631
Unique reflections	35 988	53 821	6234
Completeness (%)*	98.4 (92.9)	94.6 (89.4)	95.5 (97.6)
I/σ (%)*	25.9 (3.9)	44.6 (3.9)	10.68 (2.92)
R_{merge} (%)*†	2.5 (22.2)	2.8 (23.4)	11.1 (34.7)

Refinement data	Wild-type	A318C	Reduced C128A/D132C/K315C
Resolution (Å)	20.0–1.5	10.0–1.25	20.0–2.5
Reflections used	34 414	51 497	6099
Non-hydrogen protein atoms	1688	1577	1486
Water molecules	180	229	0
R_{free} (%)‡	22.7	22.3	27.7
R_{work} (%)§	20.5	16.6	24.1
Average B factor (Å^2)	17.7	29.2	22.9
RMSD Bonds (Å)	0.004	0.012	0.013
RMSD Angles (°)	1.24	2.30	1.71

* Number in parentheses is for outer shell.

† $R_{merge}(\%) = 100 \times \Sigma_h \Sigma_j |I_{hj} - I_h| / \Sigma_h \Sigma_j I_{hj}$ where I_h is the weighted mean intensity of the symmetry related reflections I_{hj}.

‡ R_{free} (%) is the R (%) calculated using a random selected 5% of reflection data omitted from refinement.

§ R_{work} (%) $= 100 \times \Sigma_{hkl} | F_{obs} - F_{calc} | / \Sigma_{hkl} F_{obs}$ where F_{obs} and F_{calc} are the observed and calculated structure factors respectively.

were collected on beamline 9-1 ($\lambda = 0.976$ Å) and beamline 7-1 ($\lambda = 1.08$ Å) respectively, at the Stanford Synchrotron Radiation Laboratory (Menlo Park, CA, U.S.A.). Data from the reduced C128A/D132C/K315C crystals were collected 'in-house' with an RU200 HB X-ray generator using a copper target (Cu Kα 1.542 Å). All data were processed and scaled using DENZO and SCALEPACK [25]. Molecular replacement was performed on the wild-type and mutant data sets with AMoRe [26]. The crystal structure of the wild-type closed αM-I domain (Protein Data Bank accession code 1jlm) was used as the search model for the wild-type and A318C mutant. The open αM-I domain (Protein Data Bank accession code 1IDO) was used as the search model for the reduced C128A/D132C/K315C mutant. The models were refined with CNS version 1.0 [27] using simulated annealing, positional and individual B-factor refinement alternating with manual rebuilding steps using Turbo-Frodo version 5.5 [28]. The A318C mutant was further refined with SHELX-97 [29] using positional and anisotropic B factor refinement. Final refinement and stereochemical statistics are presented in Table 1. Protein Data Bank accession codes are: 1MF7 (oxidized A318C mutant); 1NA5 (wild-type $P2_12_12_1$ crystal form) and 1N9Z (reduced C128A/D132C/K315C mutant).

RESULTS

We first made a series of single and double αM-I domain mutants based upon mutations that have been previously reported to increase the affinity of integrin $\alpha M\beta 2$ [19,30,31]. These mutations disrupt bonds between the C-terminal helix and the body of the

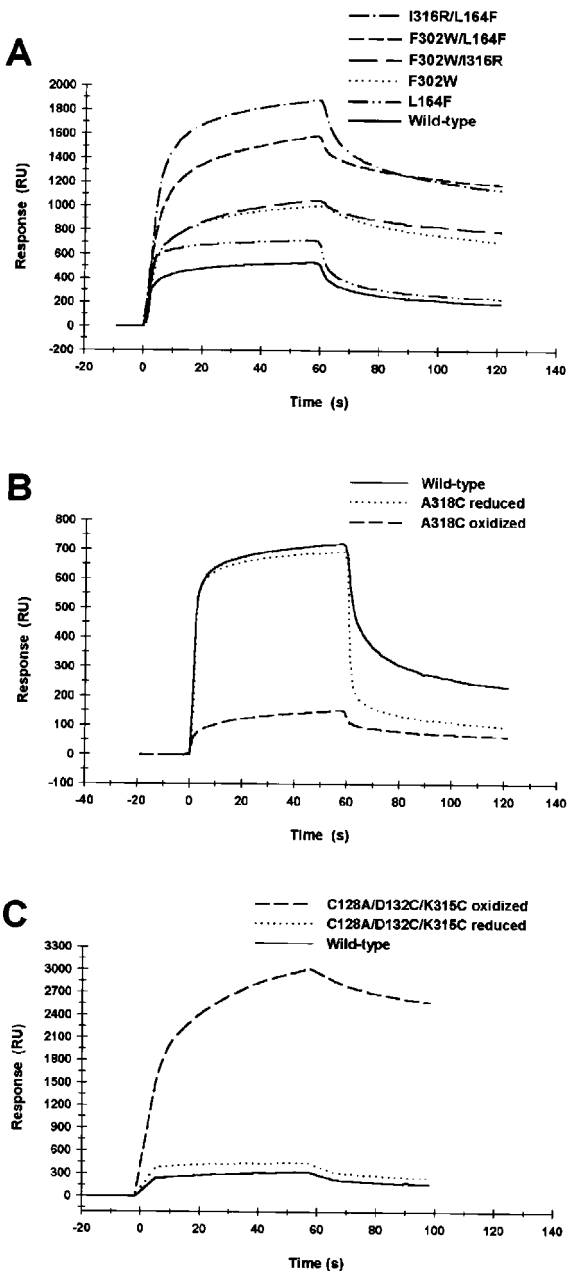

Figure 3 SPR sensorgrams of sICAM-1 and fibrinogen binding to mutant αM-I domains

(**A**) Overlays of single and double mutants: L164F, F302W, I316R/L164F, F302W/L164F, F302W/I316R and wild-type αM-I domains binding to sICAM-1. 10μM I domain was injected for 1 min at 20 $\mu l \cdot min^{-1}$ over a B1 Pioneer chip immobilized with sICAM-1. (**B**) Binding of fibrinogen to the A318C mutant. The dashed line represents the wild-type αM-I domain, the dotted line represents the mutant I domain, and the solid line represents the mutant after incubation with 10 mM DTT. (**C**) Binding of fibrinogen to the C128A/D132C/K315C triple mutant. The dashed line represents the wild-type αM-I domain, the dotted line represents the mutant I domain, and the solid line represents the mutant after incubation with 10 mM DTT. RU, response units.

domain, destabilizing the closed conformation and thus favouring the open, high-affinity conformation (Figure 1B). Except for I316R, which expressed very poorly, the mutants expressed normally and were purified as for wild-type. Binding to sICAM-1 and fibrinogen was monitored by SPR (Figure 3A). All of the mutants showed enhanced binding, but the largest increase was only 4-fold.

Table 2 K_D values for the interactions of fibrinogen and sICAM-1 with the wild-type, oxidized A318C and oxidized C128A/D132C/K315C mutant αM-I domains

$K_D \pm$ S.D. ($n = 3$).

αM-I domain type	Fibrinogen K_D (μM)	sICAM-1 (μM)
A318C mutant	25.80 ± 2.60	31.67 ± 5.32
Wild-type	3.98 ± 0.86	6.45 ± 0.58
C128A/D132C/K315C mutant	0.49 ± 0.02	0.62 ± 0.03

We made next a series of cysteine mutants that were designed to lock the conformation of the I domain, by engineering disulphide bridges between the C-terminal helix and the N-terminus. Two of these mutants expressed well and were monodisperse as judged by gel filtration; these were used for further functional and structural studies. The first mutant, A318C (Ala-318 is located at the end of the C-terminal helix), made use of the naturally occurring cysteine, Cys-128 (N-terminal to the first β-strand), as the disulphide bonding partner. The disulphide formed spontaneously as judged by lack of reactivity to DTNB, which binds to free cysteine residues. Binding to sICAM-1 and fibrinogen, as measured by SPR, was substantially (5–6-fold) reduced, compared with wild-type (Table 2). Wild-type binding was restored by reduction of the disulphide with the addition of 10 mM DTT (Figure 3B). As a control similar reducing treatment applied to the wild-type I domain had no effect on ligand binding. In order to understand this behaviour we determined the crystal structure of this mutant. Crystals grew in a space group that was different from those previously published [13,24,32], so we also grew wild-type crystals in the same space group. Both mutant and wild-type crystals diffracted X-rays to high resolution, and were closely isomorphous. We determined the structures by molecular replacement (at 1.5 Å and 1.25 Å resolution for the wild-type and mutant, respectively). The structures are very similar with a root-mean-square deviation for all Cα atoms of 0.72 Å, and represent the closed conformation as previously described [24]. The MIDAS motif is slightly distorted, so that metal does not bind; but this occurs in both wild-type and mutant structures, showing that it is a result of the intermolecular packing in this crystal form. Indeed the MIDAS of the A318C mutant is functional in solution as demonstrated by its ability to bind ligands in a cation-dependent manner. In the mutant, the N-terminal strand loops up and around the C-terminal helix to form a disulphide bond (Figure 4). This suggests that the low affinity of this mutant arises from a novel organized structure at the base of the domain, in which the N-terminal arm has wrapped around the C-terminal helix in order to form the disulphide bond, thus restraining the domain in the closed conformation by restricting the downward motion of the C-terminal helix.

The second disulphide mutant studied, the triple mutant C128A/D132C/K315C, avoided the flexibility of the residues N-terminal to the β-strand which allowed the A318C mutant to adopt the closed conformation. Asp-132 is the first residue of the N-terminal β-strand, and its main chain is held rigidly in place by being an integral part of the central β-sheet. Lys-315 lies on the C-terminal helix, one turn further upstream from Ala-318 used in the first disulphide mutant (Figure 1D). Cys-128 was mutated to alanine in order to avoid mixed disulphide formation. For this triple mutant, disulphide formation did not occur spontaneously in solution, but incubation in the presence of oxidizing agent (Cu^{2+}) allowed disulphide formation to proceed to completion. SPR analysis of the oxidized mutant revealed an approx. 10-fold

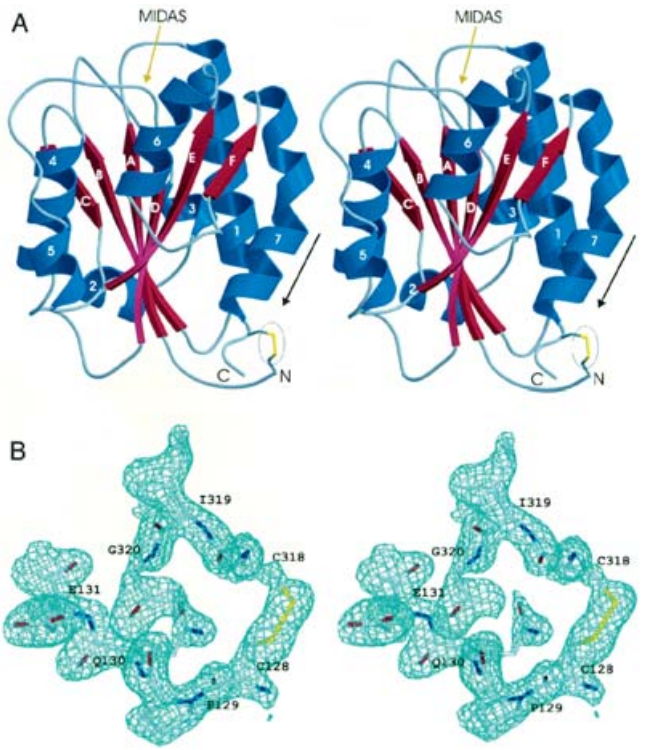

Figure 4 Crystal structure of the A318C mutant

(**A**) Stereo diagram of a ribbon representation of the A318C mutant. β-Strands are labelled A–F and helices are labelled 1–7. The disulphide bond between Cys-128 and Cys-318 is shown in yellow and circled. The direction of shift of the C-terminal helix in the transition from closed to open is shown with a black arrow. The MIDAS motif is indicated by a gold arrow. N- and C-termini are indicated. (**B**) Stereo diagram of the Cys-128–Cys-318 disulphide bond from (**A**) with the $2F_o$–F_c electron density map superimposed (contoured at 1σ). Carbon atoms are colored grey, oxygen atoms red, nitrogen atoms blue and sulphur atoms are yellow. Amino acid positions are indicated.

increase in affinity for both sICAM-1 and fibrinogen, compared with the wild-type domain (Table 2). Reduction of the disulphide reverted the domain to wild-type behaviour (Figure 3C). Typical cation dependence was observed: ligand binding was significantly reduced with EDTA treatment confirming that binding is mediated by the MIDAS.

We were unable to crystallize the triple mutant in its oxidized form, but the reduced form crystallized in the open conformation, with a ligand mimetic, and we determined its structure at 2.5 Å resolution. The structure is very similar to the wild-type open conformation [24], showing that the mutations do not unduly perturb the structure. The C-terminal helix is actually shifted by a further 2 Å 'downwards', i.e. in the closed-to-open direction. The ligand mimetic–crystal contact involves residue Glu-314, which is on the C-terminal helix next to one of the introduced cysteines. The two cysteine sulphurs are 6.5 Å apart, and modelling studies suggest that disulphide formation requires only a modest reorganization of the last turn of the C-terminal helix, which could occur readily in solution but would break the crystal contact, rationalizing the lack of growth of this crystal form under oxidizing conditions. This crystal form is, so far, unique in stabilizing the open conformation, so we made a further mutation, E314K, in order to avoid forming this crystal form. However, the oxidized quadruple mutant did not form crystals under any conditions.

DISCUSSION

Our studies show that restraining the motion of the C-terminal helix of the recombinant αM-I domain can either increase or decrease the affinity for ligand. The results are consistent for the two ligands studied, fibrinogen and sICAM-1. Restraining the helix into the 'open' conformation, by using an engineered disulphide bridge, yields an I domain that has an affinity ($K_D \approx 500$–600 nM) very similar to that of the activated parent integrin and that shows normal Mg^{2+} dependence of binding, suggesting that this conformation resembles the structure in the active integrin with an intact MIDAS motif. Although we were unable to crystallize this mutant in its oxidized form, the reduced mutant crystallized in an open conformation very similar to that observed previously for the wild-type domain. A small reorganization of the last turn of the C-terminal helix, a region that is far from the ligand-binding surface, should be sufficient to create the disulphide.

Restraining the helix to adopt the closed conformation, by using a different disulphide bridge, reduced the affinity by a factor of approx. 50-fold compared with the locked open domain. The crystal structure of this low-affinity mutant confirms that a novel disulphide bridge has formed that stabilizes the closed conformation. The bridge links an N-terminal arm to the end of the C-terminal helix. The structure is well ordered in this region (although the atomic B factors are 30–40% higher than the domain average). However, the structure suggests that a downward shift of the helix is still possible, involving a swinging motion of the N-terminal arm. This contrasts with the high-affinity mutant, in which the helix is disulphide-linked to the beginning of a β-strand that is held tightly in place as part of the central β-sheet. Thus, the affinity of a fully 'locked closed' αM-I domain is likely to be lower than that observed here. Springer and co-workers [33] recently carried out a similar series of experiments on the αL-I domain, and showed that the 'locked open' αL-I domain also has a ligand affinity comparable to that of the activated parent integrin (approx. 200 nM). They also made a 'locked closed' domain in which a disulphide bridge linked rigid elements of the domain; this displayed a ligand affinity of approx. 10^4-fold lower than the 'locked open'. Given the close structural similarities between the two domains, it is likely that a fully 'locked closed' αM-I domain would show a similar affinity reduction.

A major difference between the results for the αL and αM-I domains lies in the behaviour of the wild-type recombinant domains. In the case of αM, the wild-type ligand affinity is only approx. 10-fold less than that of the 'locked open' domain. By applying a simple thermodynamic model (Figure 5), the estimated fraction of the open conformation in the absence of ligand is 10–12%. This result is consistent with an independent estimate based on initial binding rates of αM to iC3b (the proteolytic fragment of the third component of complement) [19]. In the case of the αL-I domain, the affinity of the wild-type recombinant domain is identical to that of the 'locked closed' domain, suggesting that in solution the equilibrium between the unliganded domains is shifted almost completely ($\geqslant 10^4$) in favour of the closed conformation (Figure 5B).

How does the quaternary organization of the integrin regulate the affinity of the α-I domain? It is straightforward to build a model of the α-I domain integrin head group based on the crystal structure of $\alpha V\beta 3$ and αM-I domain (Figure 1C). The model predicts that the α-I domain will contact both the α-subunit propeller and the β-I domain. *A priori*, there are two possibilities of allosteric regulation: the quaternary organization of the inactive (resting) integrin may serve to reduce the inherent affinity of the isolated α-I domain by stabilizing its closed tertiary conformation (Model A); or the quaternary organization of the active integrin may serve to stabilize the open conformation of the I domain (Model B). The two models are not mutually exclusive, and there is evidence for both mechanisms.

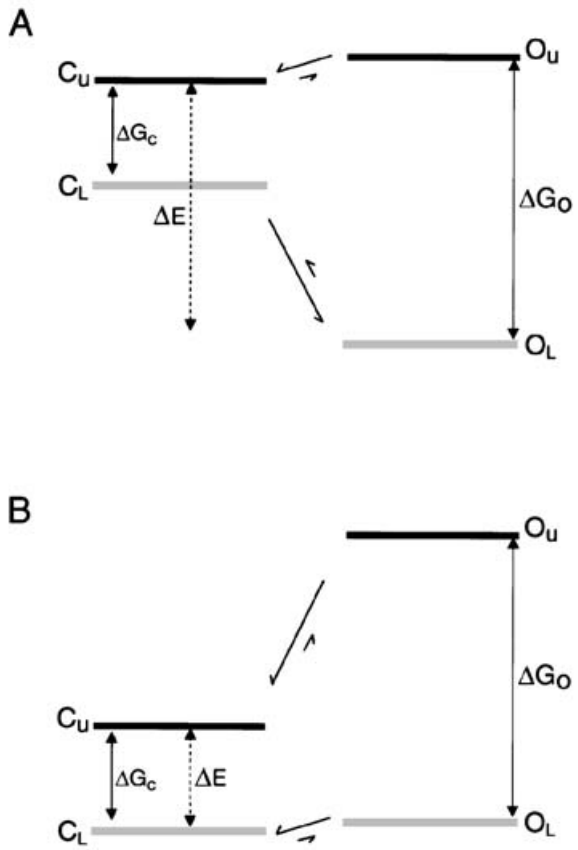

Figure 5 Energy ladders of the equilibria between open and closed conformations of αM-I and αL-I domains

(**A**) The αM-I domain. In unliganded (u) state, the equilibrium between the closed (C_U) and open (O_U) states favours the closed state by a small amount. The binding energy ($G_o = -8.7$ kCal $\cdot$ mol^{-1}) for the locked open state was measured directly by experiment on the mutant domain. The binding energy of a fully locked closed domain (ΔG_c) was not measured, but is assumed to be similar to that of αL-I. The binding energy of the wild-type domain is the population-weighted average of the binding of C_U and O_U, and approximates to ΔE. Assuming that C_L contributes negligibly to ligand binding, the observed binding energy for the wild-type domain, $\Delta G_{obs} = \Delta G_o - (1 - F)RT\ln F$, where F is the fraction of molecules in the open conformation in the absence of ligand. The two ligand-binding studies give a consistent value of $F = 0.11 \pm 0.02$, similar to that estimated from initial binding rates [19]. (**B**) The αL-I domain. Estimates of ΔG_c and ΔG_0 were obtained by experiment on disulphide-locked domains [33]. The affinity of the wild-type domain (ΔE) was identical to that of the locked closed domain. This implies that the energy of C_L is equal to or lower than that of O_L, and that the equilibrium between C_U and O_U lies greatly in favour of C_U ($F \leqslant 10^{-4}$).

Thus mutagenesis of the lower surfaces of the α-I domain has varying effects on integrin affinity. Many mutations (to both $\alpha L\beta 2$ and $\alpha M\beta 2$) are gain-of-function (Figure 1C), suggesting that these mutations disrupt intersubunit bonds that hold the α-I domain in the closed conformation, i.e., Model A [34,35]. However, a few mutations, particularly to the linker region between the C-terminal helix of α-I and the propeller, lead to loss of function [35,36]. This region includes a conserved glutamic acid, and Alonso et al. [36] have proposed that the glutamic acid completes the co-ordination sphere of the β-I domain MIDAS motif in the active integrin; that is, the active quaternary conformation serves to stabilize the open α-I domain (Model B).

As noted above, the affinity of recombinant αL-I domain is approx. 10^4-fold lower than for the locked open domain [33],

which is similar to that of the activated integrin (approx. 200 nM). The behaviour of the recombinant αL-I domain contrasts with functional studies on a recombinant soluble $\alpha L\beta 2$ integrin containing the complete extracellular head but lacking the transmembrane helices and cytoplasmic tails that stabilize the resting integrin. The affinity of this heterodimer was comparable to the locked open αL-I domain (approx. 500 nM) [35], suggesting that bonds in the active parent integrin play a similar role to the disulphide lock (Model B). An activating mutation to the inner surface of the C-terminal helix of αL-I that is predicted to destabilize the closed conformation increased affinity by a factor of 6. The energy ladder for the truncated $\alpha L\beta 2$ integrin may therefore resemble that shown for the recombinant αM-I domain (Figure 5A).

For the αM-I domain, although the affinity difference between the open and closed forms of αM is probably similar to that of αL-I (approx. 10^4), the equilibrium between the unliganded open and closed forms of the recombinant protein is much less pronounced (approx. 10^1 in favour of the closed conformer). This small energy difference (approx. 1.4 kCal $\cdot$ mol^{-1}) provides a rationale for the ability of a ligand-mimetic lattice contact to induce the open conformation of αM-I domain in the crystalline state [24]. Thus for αM-I, a major role of the integrin head appears to be to stabilize the closed conformation, so that the quaternary switch to the active state involves release of the quaternary constraints in the inactive integrin (Model A). Whether these underlying mechanistic differences have functional consequences remains to be seen.

REFERENCES

1 Hynes, R. O. (1992) Integrins: versatility, modulation, and signalling in cell adhesion. Cell (Cambridge, Mass.) **69**, 11–25
2 Xiong, J.-P., Stehle, T., Diefenbach, B., Zhang, R., Dunker, R., Scott, D. L., Joachimiak, A., Goodman, S. L. and Arnaout, M. A. (2001) Crystal structure of the extracellular segment of integrin $\alpha V\beta 3$. Science (Washington, D.C.) **294**, 339–345
3 Michishita, M., Videm, V. and Arnaout, M. A. (1993) A novel divalent cation-binding site in the A domain of the $\beta 2$ intergin CR3 (CD11b/CD18) is essential for ligand binding. Cell (Cambridge, Mass.) **72**, 857–867
4 Kamata, T. and Takada, Y. (1994) Direct binding of collagen to the I-domain of integrin $\alpha 2\beta 1$ (VLA-2, CD49b/CD29) in a divalent cation-independent manner. J. Biol. Chem. **269**, 26006–26010
5 Tuckwell, D. S., Calderwood, D. A., Green, L. J. and Humphries, M. J. (1995) Integrin $\alpha 2$ I-domain is a binding site for collagens. J. Cell Sci. **108**, 1629–1637
6 Mould, A. P., Askari, J. A., Aota, S., Yamada, K. M., Irie, A., Takada, Y., Mardon, H. J. and Humphries, M. J. (1997) Defining the topology of integrin $\alpha 5\beta 1$-fibronectin interactions using inhibitory anti-$\alpha 5$ and anti-$\beta 1$ monoclonal antibodies - Evidence that the synergy sequence of fibronectin is recognized by the amino-terminal repeats of the $\alpha 5$ subunit. J. Biol. Chem. **272**, 17283–17292
7 Hughes, P., Diaz-Gonzalez, F., Leong, L., Wu, C., McDonald, J., Shattil, S. J. and Ginsberg, M. H. (1996) Breaking the integrin hinge. J. Biol. Chem. **271**, 6571–6574
8 Takagi, J., Erickson, H. P. and Springer, T. A. (2001) C-terminal opening mimics 'inside-out' activation of integrin alpha5beta1. Nat Struct Biol. **8**, 412–416
9 Vinogradova, O., Velyvis, A., Velyviene, A., Hu, B., Haas, T., Plow, E. F. and Qin, J. (2002) A structural mechanism of integrin $\alpha IIb\beta 3$ 'inside-out' activation as regulated at its cytoplasmic face. Cell (Cambridge, Mass.) **110**, 587–597
10 Takagi, J., Petre, B. M., Walz, T. and Springer, T. A. (2002) Global conformational rearrangements in integrin extracellular domains in outside-in and inside-out signaling. Cell (Cambridge, Mass.) **110**, 599–611
11 Schwartz, M. A. and Ginsberg, M. H. (2002) Networks and crosstalk: integrin signalling spreads. Nat. Cell Biol. **4**, E65–E68
12 Garcia-Alvarez, B., de Pereda, J. M., Calderwood, D. A., Ulmer, T. S., Critchley, D. R., Campbell, I. D., Ginsberg, M. H. and Liddington, R. C. (2003) Structural Determinants of Integrin Recognition by Talin. Mol. Cell **11**, 49–58
13 Lee, J.-O., Rieu, P., Arnaout, M. A. and Liddington, R. C. (1995) Crystal structure of the A-domain from the the α subunit of integrin CR3 (CD11b/CD18). Cell (Cambridge, Mass.) **80**, 631–635
14 Kamata, T., Puzon, W. and Takada, Y. (1994) Identification of putative ligand binding sites within I domain of integrin $\alpha 2\beta 1$ (VLA-2, CD49b/CD29). J. Biol. Chem. **269**, 9659–9663
15 Kern, A., Briesewitz, R., Bank, I. and Marcantonio, E. E. (1994) The role of the I domain in ligand binding of the human integrin $\alpha 1\beta 1$. J. Biol. Chem. **269**, 22811–22816
16 Edwards, C. P., Champe, M., Gonzales, T., Wessinger, M. E., Spencer, S. A., Presta, L. G., Berman, P. W. and Bodary, S. C. (1995) Identification of amino acids in the CD11a I-domain important for binding of the leukocyte function-associated antigen-1 (LFA-1) to intercellular adhesion molecule-1 (ICAM-1). J. Biol. Chem. **270**, 12635–12640
17 Huang, C. and Springer, T. A. (1995) A binding interface on the I domain of lymphocyte function associated antigen-1 (LFA-1) required for specific interaction with intercellular adhesion molecule 1 (ICAM-1). J. Biol. Chem. **270**, 19008–19016
18 Zhang, L. and Plow, E. F. (1997) Identification and reconstruction of the binding site with in $\alpha M\beta 2$ for a specific and high affinity ligand, NIF. J.Biol.Chem. **272**, 17558–17564
19 Li, R., Rieu, P., Griffith, D. L., Scott, D. and Arnaout, M. A. (1998) Two functional states of the CD11b A-domain: correlations with key features of two Mn2+-complexed crystal structures. J. Cell Biol. **143**, 1523–1534
20 Zhang, L. and Plow, E. F. (1999) Amino acid sequences within the a subunit of integrin $\alpha M\beta 2$ (Mac-1) critical for specific recognition of C3bi. Biochemistry **38**, 8064–8071
21 Kamata, T., Liddington, R. C. and Takada, Y. (1999) Interaction between collagen and the $\alpha 2$I-domain of integrin $\alpha 2\beta 1$ - Critical role of conserved residues in the metal ion-dependent adhesion site (MIDAS) region. J. Biol. Chem. **274**, 32108–32111
22 Smith, C., Estavillo, D., Emsley, J., Bankston, L., Liddington, R. C. and Cruz, M. A. (2000) Mapping the collagen binding site in the I domain of the glycoprotein Ia/IIa (integrin $\alpha 2\beta 1$). J. Biol. Chem. **275**, 4205–4209
23 Emsley, J., Knight, C. G., Farndale, R. W., Barnes, M. J. and Liddington, R. C. (2000) Structural basis of collagen recognition by integrin $\alpha 2\beta 1$. Cell (Cambridge, Mass.) **101**, 47–56
24 Lee, J.-O., Bankston, L. A., Arnaout, M. A. and Liddington, R. C. (1995) Two conformations of the integrin A-domain (I-domain): a pathway for activation? Structure **3**, 1333–1340
25 Otwinowski, Z. and Minor, W. (1997) Processing of X-ray diffraction data collected in oscillation mode. Methods Enzymol. **276**, 307–326
26 Navaza, J. (1994) AMORE - an atomated molecular replacement program package. Acta Cryst. **A50**, 157–163
27 Brunger, A. T., Adams, P. D., Clore, G. M., DeLano, W. L., Gros, P., GrosseKunstleve, R. W., Jiang, J. S., Kuszewski, J., Nilges, M., Pannu, N. S., Read, R. J., Rice, L. M., Simonson, T. and Warren, G. L. (1998) Crystallography and NMR system: a new software suite for macromolecular structure determination. Acta Cryst. **D54**, 905–921
28 Roussel, A., and Cambillan, C. (1989) In 'Silicon Graphics Geometry Partner Directory' pp. 77–78, Silicon Graphics, Mountain View, CA., U.S.A.
29 Sheldrick, G. and Schneider, T. (1997) SHELXL: High-resolution refinement. Methods Enzymol. **277**, 319–343
30 Oxvig, C., Lu, C. and Springer, T. A. (1999) Conformational changes in tertiary structure near the ligand binding site of an integrin I domain. Proc. Natl. Acad. Sci. U.S.A. **96**, 2215–2220
31 Xiong, J. P., Li, R., Essafi, M., Stehle, T. and Arnaout, M. A. (2000) An isoleucine-based allosteric switch controls affinity and shape shifting in integrin CD11b A-domain. J. Biol. Chem. **275**, 38762–38767
32 Baldwin, E. T., Sarver, R. W., Bryant, G. L., Curry, K. A., Fairbanks, M. B., Finzel, B. C., Garlick, R. L., Heinrikson, R. L., Horton, N. C., Kelley, L. L. C., et al. (1998) Cation binding to the integrin CD11b I domain and activation model assessment. Structure **6**, 923–935
33 Shimaoka, M., Lu, C., Palframan, R. T., von Andrian, U. H., McCormack, A., Takagi, J. and Springer, T. A. (2001) Reversibly locking a protein fold in an active conformation with a disulphide bond: integrin αL I domains with high affinity and antagonist activity in vivo. Proc. Natl. Acad. Sci. U.S.A. **98**, 6009–6014
34 Zhang, L. and Plow, E. F. (1996) A discrete site modulates activation of I domains. J. Biol. Chem. **271**, 29953–29957
35 Lupher, M. L. J., Harris, E. A., Beals, C. R., Sui, L. M., Liddington, R. C. and Staunton, D. E. (2001) Cellular activation of leukocyte function-associated antigen-1 and its affinity are regulated at the I domain allosteric site. J. Immunol. **167**, 1431–1439
36 Alonso, J. L., Essafi, M., Xiong, J. P., Stehle, T. and Arnaout, M. A. (2002) Does the Integrin alphaA domain act as a ligand for its betaA domain? Curr. Biol. **12**, R340–R342
37 Liddington, R. C. and Ginsberg, M. H. (2002) Integrin activation takes shape. J. Cell Biol. **158**, 833–839

Received 12 August 2002/27 February 2003; accepted 3 March 2003
Published as BJ Immediate Publication 3 March 2003, DOI 10.1042/BJ20021273